Available online at www.sciencedirect.com
ScienceDirect
Journal of Molecular Catalysis A: Chemical 286 (2008) 92–97
JOURNAL OF MOLECULAR CATALYSIS A: CHEMICAL
www.elsevier.com/locate/molcata

Ruthenium complexes of Schiff base ligands as efficient catalysts for catechol–hydrogen peroxide reaction

Pearly Sebastian Chittilappilly [a,b], N. Sridevi [a], K. K. Mohammed Yusuff [a,*]

[a] *Department of Applied Chemistry, Cochin University of Science & Technology, Kochi 682022, India*
[b] *Department of Chemistry, St. Joseph's College, Irinjalakuda 680121, India*

Received 13 December 2007; accepted 5 February 2008
Available online 13 February 2008

Abstract

Zeolite Y-encapsulated ruthenium(III) complexes of Schiff bases derived from 3-hydroxyquinoxaline-2-carboxaldehyde and 1,2-phenylenediamine, 2-aminophenol, or 2-aminobenzimidazole (RuYqpd, RuYqap and RuYqab, respectively) and the Schiff bases derived from salicylaldehyde and 1,2-phenylenediamine, 2-aminophenol, or 2-aminobenzimidazole (RuYsalpd, RuYsalap and RuYsalab, respectively) have been prepared and characterized. These complexes, except RuYqpd, catalyze catechol oxidation by H_2O_2 selectively to 1,2,4-trihydroxybenzene. RuYqpd is inactive. A comparative study of the initial rates and percentage conversion of the reaction was done in all cases. Turn over frequency of the catalysts was also calculated. The catalytic activity of the complexes is in the order RuYqap > RuYqab for quinoxaline-based complexes and RuYsalap > RuYsalpd > RuYsalab for salicylidene-based complexes. The reaction is believed to proceed through the formation of a Ru(V) species.

Keywords: Zeolite-encapsulated complexes; Ruthenium(III); Schiff base; Catechol oxidation; Catalysis

1. Introduction

Metal complexes formed in zeolite cages can act as redox catalysts and biomimetic catalysts [1,2]. This type of catalysts possesses the advantages of both homogeneous and heterogeneous catalytic systems. Since the catalyst is trapped in zeolite cavity, products can be easily separated. Also the lifetime of the catalyst can be increased by encapsulation. Ruthenium is well known for its catalytic properties due to the fascinating electron-transfer properties [3–6]. Change in coordination environment around ruthenium plays an important role in modulating its catalytic properties. Ligands having nitrogen and oxygen donor atoms tune the properties of the complexes to a great extent as effective and stereo-specific catalysts for oxidation, reduction and hydrolysis [7–9]. But simple complexes used as catalysts cannot be recovered from the reaction system and may contaminate the products. The encapsulated copper and vanadium salen complexes in supercages of zeolite are found to be effective catalysts for the oxidation of phenol and cyclohexane [10,11]. Encapsulated copper(II) and dioxovanadium(V) complexes of Schiff bases derived from salicylaldehyde and 2-aminomethylbenzimidazole in the supercages of zeolite Y are found active for the oxidation of phenol and styrene with good conversion [12]. However, very few encapsulated complexes of ruthenium(III) are reported in literature. Considering the highly desirable attributes of zeolite-encapsulated complexes and of ruthenium(III), the present study aims at encapsulating complexes of ruthenium(III) in zeolite cages and to study their catalytic properties. With this view herein we report the preparation and characterization of zeolite-encapsulated ruthenium complexes of Schiff bases.

(a) *N*,*N*′-bis(3-hydroxyquinoxaline-2-carboxalidene)-*o*-phenylenediamine (qpd)
(b) 3-Hydroxyquinoxaline-2-carboxalidene-*o*-aminophenol (qap)
(c) 3-Hydroxyquinoxaline-2-carboxalidene-2-aminobenzimidazole (qab)
(d) *N*,*N*′-bis(salicylidene)-*o*-phenylenediamine (salpd)
(e) Salicylidene-*o*-aminophenol (salap)
(f) Salicylidene-2-aminobenzimidazole (salab)

* Corresponding author.
E-mail address: yusuff15@yahoo.com (K.K.M. Yusuff).

1381-1169/$ – see front matter © 2008 Elsevier B.V. All rights reserved.
doi:10.1016/j.molcata.2008.02.002

The catalytic potential of these complexes has been demonstrated by studying the oxidation of catechol in the presence of H_2O_2.

2. Experimental

2.1. Materials

Synthetic Y-zeolite in Na^+ form was obtained from Zeolyst International, Netherlands and reexchanged with Na^+ ions to remove any unexchanged hydrogen ions in the Zeolite matrix [13]. *o*-Phenylenediamine (Loba Chemie), 2-aminobenzimidazole (Merck), 2-aminophenol (Merck), $RuCl_3.3H_2O$ (Merck), sodium bicarbonate (Merck), catechol (Loba Chemie) and 30% H_2O_2 (Merck) were used as obtained. Solvents employed were either of 99% purity or purified by known laboratory procedures.

2.2. Physical methods and analysis

CHN analyses of the ligands and complexes were done using an elemental analyzer (Elementar model Vario EL III). The metal percentage present in the complexes were determined using ICP-AES spectrometer (Thermo Electron, IRIS Intrepid II XSP DUO). Surface area of the samples was measured by multipoint BET method (Micromeritics, Gemini 2360). Nitrogen gas was used as the adsorbate at liquid nitrogen temperature. UV–vis absorption spectra of the encapsulated complexes were recorded in Nujol by layering mull of the sample on the inside of one of the cuvettes while keeping the other one layered with Nujol as reference (Varian Cary 5000). IR spectra were recorded as KBr pellets (Schimadzu, 8000). The EPR spectra were recorded with 100 KHz field modulation at liquid nitrogen temperature (Bruker EMX X-band). Thermogravimetric analyses were done at a heating rate of 10 °C min^{-1} in nitrogen atmosphere from ambient temperature up to 1200 °C (PerkinElmer, Diamond TG/DTA). X-ray diffraction pattern of the parent zeolite and zeolite-encapsulated complexes were recorded by Bruker AXSD8 Advance diffractometer. The morphology of the samples was examined by scanning electron microscopy (JEOL, JSM-840A). The samples were dusted on alumina, coated with a thin film of gold to prevent surface charging and to protect the surface material from thermal damage by the electron beam.

2.3. Synthesis

Synthesis of the ligands was done according to the reported procedures [14,15].

2.3.1. Preparation of ruthenium exchanged zeolite (RuY)

NaY (5.0 g) was stirred with ruthenium(III) chloride solution (0.001 M, 250 mL) at 70 °C for 4 h. The slurry was filtered and washed with deionised water to make it free from anions. It was then dried at 120 °C for 1 h and then at 450 °C for 4 h.

2.3.2. Synthesis of Ru(III) zeolite-encapsulated complexes of qpd, qap, qab, salpd, salap and salab

Ruthenium(III) exchanged zeolite, RuY (5.0 g) was added to a solution of the ligand in ethanol (50 mL), the concentration of ligand in the solution being at equal mole ratio to the metal ion. The mixture was refluxed for 10 h to ensure complexation. The resultant mass was filtered and soxhlet extracted with methanol until the extracting solvent became colourless. It was further soxhlet extracted with acetone to ensure complete removal of the surface species. The uncomplexed metal ions in the zeolite and ionisable portions of the ligand were removed by ion exchange with NaCl solution (0.01 M, 250 mL) for 24 h. It was filtered, washed free of chloride ions and finally dried at 100 °C for 2 h and stored in vacuum over anhydrous calcium chloride.

2.4. Catalytic oxidation of catechol

Catechol (1.0×10^{-2} mol dm^{-3}) solution was prepared in methanol afresh before each kinetic run. The stock solution of H_2O_2 was prepared before each set of kinetic runs by diluting 10 mL of 30% H_2O_2 to 100 mL. It was standardized permanganometrically.

All kinetic runs were carried out at 28.0 ± 0.1 °C in 9:1 methanol–water mixtures. To carry out the reaction catechol solution (9 mL) was mixed with the catalyst (0.01 g) and the reaction was initiated by adding H_2O_2 solution (1 mL). The blank used was a mixture of methanol (9 mL) and water (1 mL). In order to identify the products, the spectrum of the reaction mixture was obtained after completion of the reaction. No peak was observed at 390 nm corresponding to the formation of *o*-benzoquinone [16] while a new peak corresponding to 1,2,4-trihydroxybenzene was noticed in the product spectrum showing that the reaction is selective towards the formation of 1,2,4-trihydroxybenzene. The progress of the reaction was monitored spectrophotometrically at an interval of 1 min by measuring the absorbance at 290 nm [17] and also at a second wavelength at which catechol and the product of the reaction do not absorb. The absorbance measured at the later wavelength corresponds to the scattering due to the catalyst particles. To get the actual absorbance of the product, the absorbance due to scattering was deducted from the absorbance at 290 nm [18]. The catalysis of RuY in the present reaction was verified at identical conditions and found to be absent.

The catalytic activities of the complexes were compared using initial rates of the reaction. Initial rates were obtained by fitting the concentration–time data into the polynomial of the form $[C] = a_0 + a_1 t + a_2 t^2 + \cdots$ where C and t represent concentration and time, respectively. a_0, a_1, a_2, etc. are constants. The coefficient of 't' gives the initial rate [19]. This was done using Microsoft Excel.

3. Results and discussion

3.1. Characterization of catalysts

Elemental analysis (Table 1) of NaY revealed a Si/Al ratio of 2.6 that corresponds to a unit cell formula

Table 1
Analytical data of metal exchanged zeolites and encapsulated complexes

Sample	Elements %found						
	%C	%H	%N	%Ru	%Si	%Al	%Na
NaY	–	–	–	–	20.9	7.9	9.6
RuY	–	–	–	1.8	20.4	7.6	5.6
RuYqpd	0.98	2.63	0.05	0.3	20.1	7.4	7.8
RuYqap	0.82	1.51	0.03	0.4	19.9	7.7	8.2
RuYqab	1.10	2.58	0.23	0.9	19.6	7.4	3.9
RuYsalpd	0.85	2.61	0.05	0.3	20.3	7.5	8.1
RuYsalap	1.03	2.70	0.05	0.6	20.1	7.4	7.1
RuYsalab	1.80	2.54	0.27	0.5	20.2	7.6	6.1

Table 2
Surface area and pore volume data

Sample	Surface area (m^2/g)	Pore volume (cc/g)
Zeolite	799	0.3978
NaY	692	0.3482
RuY	682	0.3458
RuYqpd	627	0.3195
RuYqap	482	0.2369
RuYqab	567	0.2920
RuYsalpd	662	0.3367
RuYsalap	627	0.3266
RuYsalab	662	0.3520

$Na_{54}(AlO_2)_{54}(SiO_2)_{138}{\cdot}nH_2O$ for NaY [20]. Almost constant value of Si/Al ratio was found even after the metal exchange and formation of complexes confirming the retention of the zeolite framework during complexation. The unit cell formula of ruthenium exchanged zeolite was derived to be $Na_{44.14}Ru_{3.29}(AlO_2)_{54}\,(SiO_2)_{138}{\cdot}nH_2O$ from the metal percentage of RuY. This correspond to18.3% as the degree of ion exchange. The elemental analysis confirms the presence of metal complexes in the zeolite matrix.

Surface area analysis of the complexes indicated a small reduction in surface area (Table 2) due to metal exchange and complex formation. Such a reduction in surface area and pore volume due to complex formation is generally attributed to filling the pore [2].

TG/DTG curves show that the pattern of decomposition is the same for all encapsulated complexes. DSC curve shows endothermic peak corresponding to the deaquation of the sample around 100 °C which is followed by an exothermic maxima corresponding to the decomposition of the encapsulated complex. The thermogravimetric data of the encapsulated complexes are given in Table 3.

IR spectra of the complexes after heating to 150 °C exhibited similar peaks as that of original complex, indicating that complex is not decomposed till 150 °C. The decomposition stage found immediately after 200 °C in all complexes exhibited very small percentage of weight loss (∼7%) which might be due to the decomposition of the complex within the zeolite cage.

Zeolite framework retains its crystallinity even after encapsulation, which is evidenced by the similar X-ray diffraction patterns of the RuY and metal complex encapsulated zeolite. This supports the fact that reduction in surface area observed is not due to collapse of crystalline structure but due to encapsulation of complexes in the cages.

Scanning electron micrographs of encapsulated complexes [21] before and after Soxhlet extraction were taken which shows that surface species formed during complexation were completely removed by Soxhlet extraction.

The infrared band around 1640 cm^{-1} in the ligand is shifted to lower frequencies in all the zeolite-encapsulated complexes, which confirms complexation at nitrogen of the azomethine group (Table 4). Band at 3461 cm^{-1} in qab and at 3470 cm^{-1} in salab are due to N–H of imidazole ring. These experience slight shift towards lower frequencies in RuYqab and RuYsalab, respectively which can be attributed to changes in environment due to coordination at other positions. IR spectra of all zeolite-encapsulated complexes show bands in the region 1500–1570 cm^{-1}. These are assigned to C–C stretching vibrations of benzene ring. Since there are no zeolite bands at this position, ν_{C-C} of benzene ring suggests encapsulation of complexes.

In the IR spectra of the free ligands, bands occur in the region 1270–1300 cm^{-1} due to ν_{C-O} of phenolic group. However, this is absent in encapsulated complexes. This might be due to the masking by the broad zeolite band around 1000 cm^{-1}. A sharp band is seen in all encapsulated complexes between 1020 and 1030 cm^{-1}which is not seen in the corresponding ligands. Hence, it can be assigned to the zeolite framework vibration. Other major zeolite framework bands appear around 1140, 725 cm^{-1} [22]. Also most of the bands due to ligands are masked by the zeolite peaks in complexes. However the bands due to azomethine group could be observed with shifts towards lower frequencies.

The electronic spectral data of the encapsulated complexes are given in Table 5. It has been reported that in a number of

Table 3
TG/DTG data of encapsulated complexes

Compound	I stage		II stage	
	Weight loss till 200 °C (%)	Peak temperature (°C)	Temperature range (°C)	Weight loss (%)
RuYqpd	28	106	200–800	8
RuYqap	21	101	200–600	6
RuYqab	25	115	200–550	7
RuYsalpd	28	113	200–550	6
RuYsalap	28	107	200–550	9
RuYsalab	28	108	200–550	8

Table 4
IR spectral data of ligands and zeolite-encapsulated complexes

Compound	ν_{N-H}	ν_{O-H}	ν_{C-O} of phenolic group	$\nu_{C=N}$ of azomethine group	ν_{C-C} stretching	$\nu_{zeolitic\ peaks}$	$\nu_{zeolite\ peaks}$	$\nu_{coord\ water}$
qpd		3474	1275	1651	1534			
RuYqpd		3459		1640	1526	1021	579	789
qap			1280	1630	1525			
RuYqap		3448		1621	1513	1026	580	782
qab	3461		1283	1642	1530			
RuYqab	3452			1635	1507	1024	571	808
salpd			1275	1651	1561			
RuYsalpd		3489		1644	1547	1023	579	792
salap			1273	1639	1526			
RuYsalap		3439		1630	1518	1023	579	785
salab	3470		1278	1641	1533			
RuYsalab	3459			1636	1520	1023	576	792

ruthenium complexes charge transfer absorptions occur at relatively low energies. In the present complexes the high intensity transitions above 30,000 cm^{-1} are assigned as charge transfer bands [23,24]. The ground state for the low spin octahedral complexes is $^2T_{2g}$ and the excited states are $^2A_{2g}$, $^2T_{1g}$, ^2E_g. In RuYqpd, the absorption peak seen as shoulder on the high intensity charge transfer band at 28490 cm^{-1} is assigned to the transition $^2T_{2g} \rightarrow {}^2A_{2g}$, $^2T_{1g}$. As the crystal field parameters are quite large, the expected electronic transition, $^2T_{2g} \rightarrow {}^2E_g$, usually occur in the region of absorptions of the charge transfer bands and are frequently obscured in some complexes [25]. However, the spin forbidden transition, $^2T_{2g} \rightarrow {}^4T_{1g}$, is frequently observed in some of the octahedral complexes. The bands occurring in the region 17,000–17,600 cm^{-1} have been assigned to the spin forbidden transitions [25,26]. The values suggest octahedral geometry for the complexes.

EPR spectrum of encapsulated complex RuYsalap gives three *g* values (Table 6) indicating rhombohedral distortion of octahedral geometry. RuYqab and RuYsalab present an axial symmetry giving two *g* values. A well-resolved EPR spectrum could not be obtained for the other complexes.

Table 5
Electronic spectral data of the encapsulated complexes of ruthenium

Complex	Absorbance (cm^{-1})	Tentative assignments
RuYqpd	34,720	Charge transfer
	28,490 (sh)	$^2T_{2g} \rightarrow {}^2A_{2g}$, $^2T_{1g}$
	17,540	$^2T_{2g} \rightarrow {}^4T_{1g}$
RuYqap	20,620	$^2T_{2g} \rightarrow {}^2E_g$
	17,480	$^2T_{2g} \rightarrow {}^4T_{1g}$
RuYqab	34,600	Charge transfer
	29,470 (sh)	$^2T_{2g} \rightarrow {}^2A_{2g}$, $^2T_{1g}$
	20,700	$^2T_{2g} \rightarrow {}^2E_g$
	17,570	$^2T_{2g} \rightarrow {}^4T_{1g}$
RuYsalpd	36,100	Charge transfer
	33,350 (sh)	$^2T_{2g} \rightarrow {}^2A_{2g}$, $^2T_{1g}$
RuYsalap	36,630	Charge transfer
	34,360 (sh)	$^2T_{2g} \rightarrow {}^2A_{2g}$, $^2T_{1g}$
	20,280	$^2T_{2g} \rightarrow {}^2E_g$
RuYsalab	36,000	Charge transfer
	28,490 (sh)	$^2T_{2g} \rightarrow {}^2A_{2g}$, $^2T_{1g}$
	17,270	$^2T_{2g} \rightarrow {}^4T_{1g}$

Table 6
EPR spectral parameters of zeolite encapsulated complexes

Sample	EPR parameters
RuYqab	$g_{\|\|} = 2.12$; $g_\perp = 2.14$
RuYsalap	$g_1 = 2.17$; $g_2 = 2.12$; $g_3 = 2.00$
RuYsalab	$g_{\|\|} = 2.16$; $g_\perp = 2.05$

3.2. Comparison of catalytic activity of the encapsulated complexes of ruthenium

The reaction was found to be selective towards the formation of 1,2,4-trihydroxybenzene in the presence of encapsulated complexes of ruthenium(III). The plots of absorbance versus time are shown in Figs. 1 and 2. The initial rates obtained during the catalytic activity studies of the synthesized complexes are presented in Table 7. The percentage conversion of catechol to 1,2,4-trihydroxybenzene in 30 min and TOF (h^{-1}) were also calculated and are presented in Table 7. Of all the synthesized Schiff base complexes the one derived from *o*-aminophenol was found to be the most active. The oxidation of Ru(III) by H_2O_2 might be proceeding through the formation of Ru(V) species, which is then reduced by catechol to Ru(III). IR studies of these

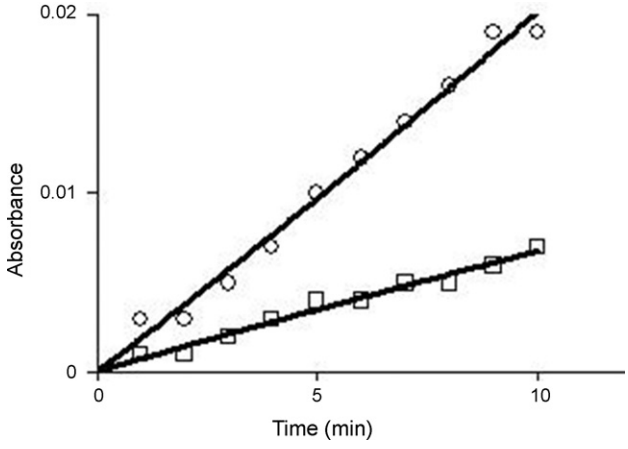

Fig. 1. Kinetic plot of absorbance versus time for catechol–H_2O_2 reaction catalyzed by (◯) RuYqap and (□) RuYqab.

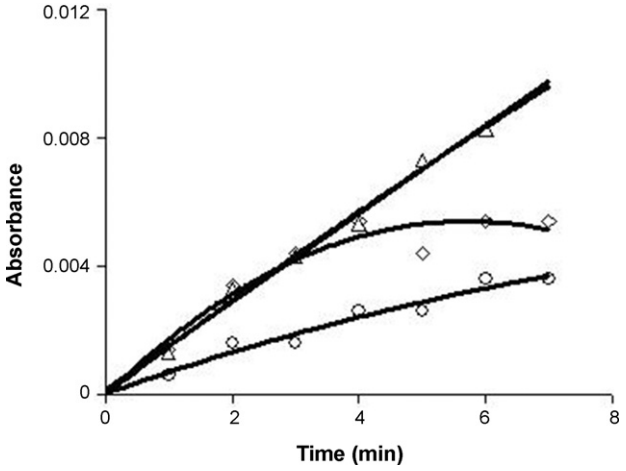

Fig. 2. Kinetic plot of absorbance versus time for catechol–H_2O_2 reaction catalyzed by (△) RuYsalab, (□) RuYsalap and (◯) RuYsalpd.

Table 7
Initial rates and percent conversion of catechol–H_2O_2 reaction using encapsulated complexes of ruthenium as catalyst

Catalyst	Initial rate/unit weight of ruthenium × 10^4 (mol dm^{-3} s^{-1})	Conversion% in 30 min	TOF (h^{-1})[a]
RuYqpd	–	–	–
RuYqap	18.6	6.4	3232
RuYqab	3.0	2.8	628
RuYsalpd	9.1	2.2	1481
RuYsalap	12.4	9.2	3097
RuYsalab	8.6	2.1	848

[Catechol] = 1×10^{-2} mol dm^{-3}, [H_2O_2] = 1×10^{-2} mol dm^{-3}.
[a] TOF (h^{-1}) = no. of moles of substrate converted per mole of catalyst in 1 h.

complexes showed that salap binds through one imino nitrogen, salpd binds through two imino nitrogens and salab binds to the metal atom through one imino nitrogen. The increase in activity of the RuYsalap complex might be due to the coordination of the phenolato oxygen atoms which makes the metal centre more electron rich, hence can be oxidized more easily to the +5 state than the complexes derived from 1,2-phenylenediamine and 2-aminobenzimidazole.

RuYqpd remained inactive for reasons unknown. In the presence of RuYqap 6.4% conversion was achieved in 30 min with a TOF (h^{-1}) of 3232. RuYqab complex shows activity with lesser percent conversion and TOF. The catalytic activity of the salicylidene complexes are in the order RuYsalap > RuYsalpd > RuYsalab.

4. Conclusion

New zeolite-encapsulated Ru(III) complexes of Schiff bases have been synthesized and characterized. The integrity of encapsulation was confirmed by spectroscopic studies as well as chemical, surface area and thermal analysis. The similarity in XRD pattern of NaY, RuY and encapsulated complexes revealed that the framework retains its crystal structure even after complexation. The removal of surface species was ascertained by SEM analyses. The lower surface area and pore volume of complexes as compared to metal exchanged zeolite suggest encapsulation. The coordination of ligands with metal ion was ascertained in all cases by IR spectra. On the basis of magnetic moment, electronic spectra and EPR, an octahedral geometry was suggested for all the complexes. These complexes, except qpd complex, catalyze catechol oxidation by H_2O_2 selectively to 1,2,4-trihydroxybenzene. Encapsulated complex of qpd is inactive. A comparative study of the initial rates, percentage conversion and turn over frequency of the reaction was done in all cases. The catalytic activity of the complexes is in the order RuYqap > RuYqab for quinoxaline-based complexes and RuYsalap > RuYsalpd > RuYsalab for salicylaldene-based complexes.

Acknowledgements

One of the authors (P.S.C) is thankful to University Grants Commission, New Delhi for the financial support in the form of research project. The authors thank Department of Science and Technology, India, for using the Sophisticated Analytical Instrumentation Facility (SAIF) at IIT Bombay for the EPR spectral data and at the Sophisticated Test & Instrumentation Centre, Cochin University of Science and Technology for the elemental analyses.

References

[1] R. Raja, P. Ratnasamy, J. Mol. Catal. A: Chem. 100 (1995) 93–102.
[2] K.J. Balkus Jr., A.G. Gabrielov, J. Inclusion Phenom. Mol. Recogn. Chem. 21 (1995) 159–184.
[3] (a) K.R. Seddon, Coord. Chem. Rev. 35 (1981) 41–83;
(b) K.R. Seddon, Coord. Chem. Rev. 41 (1982) 79–157;
(c) K.R. Seddon, Coord. Chem. Rev. 67 (1985) 171–242.
[4] W.T. Wong, Coord. Chem. Rev. 131 (1994) 45–94.
[5] B.K. Ghosh, A. Chakravorty, Coord. Chem. Rev. 95 (1989) 239–294.
[6] K. Kalyansundaram, Coord. Chem. Rev. 46 (1982) 159–244.
[7] R.I. Kureshy, N.H. Khan, S.H.R. Abdi, S.T. Patel, P. Iyer, J. Mol. Catal. A: Chem. 150 (1999) 175–244.
[8] Y.K. Aoyama, T. Fujisawa, T. Walanabe, H. Toi, H. Ogashi, J. Am. Chem. Soc. 108 (1986) 943–947.
[9] R.S. Brown, M. Zamkanei, J.L. Cocho, J. Am. Chem. Soc. 106 (1984) 5222–5228.
[10] C.R. Jacob, S.P. Varkey, P. Ratnasamy, Appl. Catal. A: Gen. 168 (1997) 353–364.
[11] M.R. Maurya, M. Kumar, S.J.J. Titinchi, H.S. Abbo, S. Chand, Catal. Lett. 86 (2003) 97–105.
[12] M.R. Maurya, A.K. Chandrakar, S. Chand, J. Mol. Catal. A: Chem. 263 (2006) 227–237.
[13] E.H. Yonemoto, Y.I. Kim, R.H. Schmchl, J.O. Wallin, B.A. Shoulders, B.R. Richardson, J.F. Haw, T.E. Mallouk, J. Am. Chem. Soc. 116 (1994) 10557–10563.
[14] S. Sailaja, M.R. Reddy, K.M. Raju, K.H. Reddy, Indian J. Chem. 38A (1999) 156–160.
[15] J. Mathew, Ph.D. Thesis, Cochin University of Science and Technology (1995).
[16] A.L. Abuhijleh, C. Woods, E. Bogas, G.L. Guenniou, Inorg. Chim. Acta 195 (1992) 67–71.
[17] Y. Tao, A. Fishman, W.E. Bentley, T.K. Wood, Appl. Environ. Microbiol. 70 (2004) 3814–3820.
[18] N.R. Suja, N. Sridevi, K.K.M. Yusuff, Kinet. Catal. 45 (2004) 337–344.

[19] S. Mayadevi, N. Sridevi, K.K.M. Yusuff, Indian J. Chem. 37A (1998) 413–417.
[20] K.O. Xavier, J. Chacko, K.K.M. Yusuff, J. Mol. Catal. A: Chem. 178 (2002) 275–281.
[21] J.M. Thomas, C.R.A. Catlow, Prog. Inorg. Chem. 35 (1988) 1–49.
[22] T.A. Egerton, A. Hagan, F.S. Stone, J.C. Vickerman, J. Chem. Soc. Faraday Trans. 1 68 (1972) 723–735.
[23] W.W. Holloway Jr., M. Kestigian, Spectrochim. Acta 22 (1966) 1381–1382.
[24] D. Wester, R.C. Edwards, D.H. Bush, Inorg. Chem. 16 (1977) 1055–1060.
[25] A.B.P. Lever, Inorganic Electronic Spectroscopy, 2nd ed., Elsevier, Amsterdam, 1984.
[26] G.C. Allen, G.A.M. El-Sharkawy, K.D. Warren, Inorg. Chem. 12 (1973) 2231–2237.